

Alkyl Chain Size Effects on Liquid Phase Properties of 1-Alkyl-3-Methylimidazolium Tetrachloroaluminate Ionic Liquids—A Microscopic Point of View from Computational Chemistry

Jones de Andrade, Elvis S. Böes, and Hubert Stassen*

Grupo de Química Teórica, Instituto de Química, Universidade Federal do Rio Grande do Sul Av. Bento Gonçalves 9500, 91540-000, Porto Alegre - RS, Brazil

Received: February 16, 2009; Revised Manuscript Received: April 3, 2009

Microscopic insights for effects of the alkyl chain length on macroscopic physical properties of 1-alkyl-3-methylimidazolium ionic liquids are provided from molecular dynamics computer simulation and quantum mechanical calculations. In particular, the liquid densities, internal energies, and hydrogen bonding behavior of the ions were studied. The effect of the alkyl chain size on the hydrogen bonding behavior of these liquids, in terms of both radial distribution functions and pair energetics, is demonstrated. Finally, studies of the ion pair stabilization were performed at the quantum mechanical level by means of the Kitaura–Morokuma energy partition. The fitting of atomic charges to the ion pairs has been performed to illustrate the charge transfer effect between cation and anion.

1. Introduction

In the last decades, both the public concern and the rigorous legislations on environmental awareness and protection of natural resources guided Chemistry toward the so-called Green Technologies.¹ In particular, the substitution of common organic solvents by supercritical fluids,² perfluorinated solvents,³ or room temperature molten salts (ionic liquids, ILs)⁴ has attracted remarkable research interest. Among these Green solvents, the ILs are being explored in a variety of chemical syntheses⁵ for several reasons: Most of them are nonvolatile solvents with rare exceptions that possess very low vapor pressures,^{6–8} represent good solvents for a large number of chemical substances, and can be customized for chemical applications by the choice of particular cations and anions.

Experimental studies describing physical–chemical phenomena in ILs have been the focus of an increasing number of publications.⁹ In addition, methodologies from computational chemistry, most of them exploiting molecular dynamics (MD) techniques or quantum mechanical (QM) approaches, have been employed in detailed studies on ILs.^{10–12} In particular, our group has published an all-atom flexible force field for 1-alkyl-3-methylimidazolium based ILs^{13–15} within the parameter development scheme for the AMBER force field.¹⁶ This potential model has been validated against the experimental neutron structure factor for the IL composed by 1-ethyl-3-methylimidazolium ($C_2C_1mim^+$) cations and tetrachloroaluminate ($AlCl_4^-$) anions¹³ and extended to include also the 1-butyl-3-methylimidazolium ($C_4C_1im^+$) cation and tetrafluoroborate (BF_4^-) anion.¹⁴

Recently, we elucidated the anion size effect on the local structure of the ILs¹⁷ from MD simulations. In the present manuscript, we focus on the effect of alkyl chain size on the properties of the ILs. For this reason, we extended our force field and included two new cations: 1,3-dimethylimidazolium ($C_1C_1im^+$) and 1-propyl-3-methylimidazolium ($C_3C_1im^+$). Thus, performing MD simulations, we are able to compare the chain length effect for the 1-alkyl-3-methylimidazolium ($C_nC_1im^+$)

cations with $n = 1, 2, 3, 4$ on properties such as density, internal energy, structural parameters, electrostatic properties, and hydrogen bonding. In any case, we have chosen $AlCl_4^-$ as the counterion.

Experimentally^{18,19} and from MD simulations,^{20–23} alignments of alkyl groups have been observed in dialkylimidazolium based ILs. This tail aggregation becomes stronger with increasing side chains. For very long alkyl groups, liquid crystals composed by dialkylimidazolium based ILs have been characterized.^{24–27} If one assumes that most of the cation's charge is localized within the imidazolium ring skeleton, the alkyl side chains can be considered as almost electrostatically neutral. Thus, the alkyl chains represent groups dominated by van der Waals type interactions. MD simulations have demonstrated that the contribution of the van der Waals interaction energy in these ILs increases when the side chains are augmented.²³

Several recent publications have been directed toward the effect of polarization and charge transfer effects in imidazolium based ILs. Liquid state properties for the IL $C_2C_1imNO_3$ computed from MD simulations are in better agreement with experimental findings when polarization interactions are considered.²⁸ Similar improvements have been observed in physical–chemical properties when an effective dielectric constant is introduced into the Coulomb part of the classical force field utilized in MD simulations on the IL containing $C_4C_1im^+$ cations and bis(trifluoromethylsulfonyl)imide anions,²⁹ or when atomic point charges are somewhat scaled down.^{30,31} In the present manuscript, we investigate the effect of polarization and modified electrostatic interactions between cations and anions at the QM level. Therefore, we performed ab initio calculations on isolated ion pairs and analyzed the energetic situation of the pairs in terms of the Kitaura–Morokuma partition scheme.³²

2. Methods

In the present study, we have employed several computational techniques. The liquid state properties have been obtained from classical MD simulations. QM calculations were necessary for

* To whom correspondence should be addressed. E-mail: gullit@iq.ufrgs.br.

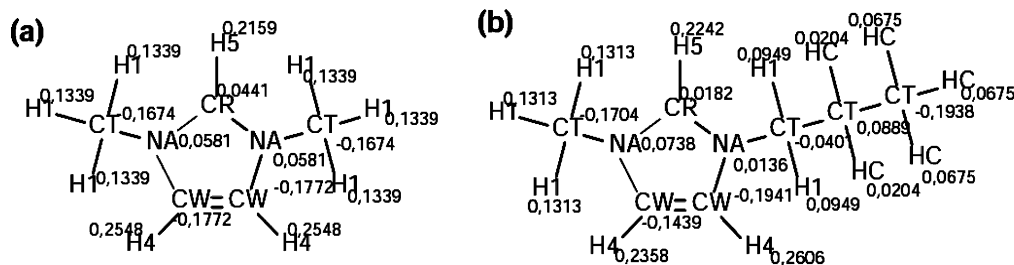


Figure 1. Amber atom types and computed point charges for the $C_1C_1im^+$ (a) and $C_3C_1im^+$ (b) cations.

the parametrization of the force field for the $C_3C_1im^+$ and $C_1C_1im^+$ cations. Molecular mechanics (MM) has been applied to verify the established force field parameters for the cations. In addition, QM calculations on the ion pairs for all of the cations with the $AlCl_4^-$ anion have been performed. In this section, we describe the computational details.

QM Calculations on Isolated Cations. The cations $C_3C_1im^+$ and $C_1C_1im^+$ were treated quantum mechanically with the PC-GAMESS program³³ at the RHF/6-31G(d) level of theory. Note that the choice of this particular basis set is recommended for the parameter development in the AMBER force field.¹⁶ The calculation included the geometry optimization for both cations furnishing bond lengths, bond angles, and dihedral angles. A Hessian matrix diagonalization has been performed to obtain the normal modes for the two cations. The electrostatic potential (ESP) grid was generated and subsequently utilized by the one-conformation two-step fitting of RESP charges performed by the RESP program from the AMBER package.³⁴

QM Calculations on Ion Pairs. For the ion pair studies, we employed ab initio calculations at the RHF/6-31G(d), RHF/6-31G(d,p), and RHF/6-311G(d,p) levels. We performed geometry optimizations, bond order analysis, and the charge fitting procedure described above. Additionally, we applied the Kitaura–Morokuma interaction energy partition³² to study the ion pairs. This method for analyzing the interaction energy between molecules is particularly useful for the study of the interaction between cations and anions of the ILs. According to the Kitaura–Morokuma approach, at the Hartree–Fock level of theory, the interaction energy E_{A-B} between molecules A and B can be decomposed into various contributions

$$E_{A-B} = E_{ES} + E_{EX} + E_{PL} + E_{CT} + E_{Mix} \quad (1)$$

where E_{ES} represents the interaction energy of the two charge distributions, E_{EX} the exchange-repulsion energy, E_{PL} the polarization energy, E_{CT} the contribution originated at charge transfers, and E_{Mix} a portion resulting from higher order coupling of the various terms.

In more detail, the exchange-repulsion term stems from the exchange and overlap integrals for the interacting molecules A and B. The overlap between the occupied molecular orbitals of the two molecules represents a repulsive interaction (positive sign) that is usually stronger than the attractive (negative sign) contribution from the exchange integrals. The polarization energy is defined as the energetic contribution from the field created by the charge distribution of one molecule disturbing the charge distribution of the other, and vice versa. Thus, E_{PL} contains the polarization in molecule A ($E_{PL,A}$), the polarization in molecule B ($E_{PL,B}$), and an additional contribution $E_{PL,Mix}$ originated at simultaneous polarization of A and B. The possibility of transferring electron density from occupied molecular orbitals of one molecule into unoccupied molecular orbitals of the other defines the charge transfer process. Thus, E_{CT} is given by the sum of the energy related to the charge

transfer from A to B ($E_{CT,A}$) as well as the charge transfer from B to A ($E_{CT,B}$).

MM Calculations. MM calculations have been performed for the isolated cations using the established force field parameters. We have carried out geometry optimizations and normal-mode analysis by the MINIMIZE and VIBRATE programs of the Tinker package.³⁵ The corresponding bond lengths, bond angles, and dihedrals were computed for comparison with the QM results and data from the liquid phase MD simulations. The MM normal modes were computed in order to verify and eliminate larger deviations in the vibrational frequencies introduced by the classical force field when compared to the QM results.

MD Simulations on the ILs. The MD simulations were carried out with the MDynaMix program.³⁶ Further trajectory analysis was performed by self-written programs. All of the results presented here were obtained from simulations in the NpT ensemble (Nosé–Hoover thermo- and barostat,³⁷ coupling constants of 30 and 400 fs, respectively). The applied temperatures and pressures (1 atm) correspond to thermodynamic states with experimental data available for the liquid density.

The simulation box was composed of 128 randomly arranged ion pairs, under periodic boundary conditions. The double time-step algorithm of Tuckerman and Berne³⁸ was used for the numerical integration of the equations of motion. The large time step was kept at 2 fs and the shorter at 0.2 fs. The equilibration period was extended to at least 200 ps, and the production runs lasted not less than 100 ps. Liquid configurations were saved for further analysis in intervals of five integration time steps (10 fs). In all of the simulations, the cutoff radius was fixed at 17 Å, also representing the real-space cutoff radius for the Ewald summation³⁹ utilized for computation of long-range Coulombic interaction energies and forces.

The equilibration phase was monitored by plotting the total, kinetic, intermolecular, and intramolecular energies. From the production runs, we computed the average densities ρ , internal energies U , and radial distribution functions (RDFs). U has been separated into the electrostatic U_{el} and van der Waals U_{vdw} contributions.

The $C_2C_1im^+$ and $C_4C_1im^+$ cations as well as the $AlCl_4^-$ anions were modeled with our previously established force field.^{13,14} The parametrization procedures outlined in these references have been employed to extend the force field to the $C_1C_1im^+$ and $C_3C_1im^+$ cations. The choice of the atom types for the new cations are shown in Figure 1. The corresponding IUPAC nomenclature for the imidazolium atoms is illustrated in Figure 2.

In the MD simulations, we utilized, as mentioned above, the AMBER potential model

$$V = \sum_{\text{bonds}} K_r(r - r_{\text{eq}})^2 + \sum_{\text{angles}} K_\theta(\theta - \theta_{\text{eq}})^2 + \sum_{\text{dihedrals}} \frac{V_n}{2}[1 + \cos(n\phi - \gamma)] + \sum_{i=1}^{N-1} \sum_{j>i}^N \left[\frac{A_{ij}}{R_{ij}^{12}} - \frac{B_{ij}}{R_{ij}^6} + \frac{q_i q_j}{R_{ij}} \right] \quad (2)$$

with all of the variables and parameters possessing their usual meaning.¹⁶ To achieve compatibility with the MDynaMix program, the nonbonded parameters A_{ij} and B_{ij} were expressed in terms of the traditional Lennard-Jones size σ_{ij} and well-depth ϵ_{ij} parameters

$$A_{ij} = 4\epsilon_{ij}\sigma_{ij}^{12} \quad (3)$$

$$B_{ij} = 4\epsilon_{ij}\sigma_{ij}^6 \quad (4)$$

with the usual Lorentz–Berthelot mixing rules applied to the parameters for interactions between unlike atom types

$$\epsilon_{ij} = \sqrt{\epsilon_i \epsilon_j} \quad (5)$$

$$\sigma_{ij} = \frac{1}{2}(\sigma_i + \sigma_j) \quad (6)$$

3. Results and Discussion

3.1. $\text{C}_1\text{C}_1\text{im}^+$ and $\text{C}_3\text{C}_1\text{im}^+$ Models. The atomic point charges for the two new cations, $\text{C}_1\text{C}_1\text{im}^+$ and $\text{C}_3\text{C}_1\text{im}^+$, obtained from the RESP fitting procedure are presented in Figure 1. Comparing the numerical values of the point charges for the two cations from Figure 1 with the $\text{C}_2\text{C}_1\text{im}^+$ ¹³ and $\text{C}_4\text{C}_1\text{im}^+$ ¹⁴ cations, we observe a very similar charge distribution in the imidazolium ring for the four cations.

With respect to the other intra- and intermolecular potential parameters from eq 2, we utilized the previously established set of parameters for the $\text{C}_2\text{C}_1\text{im}^+$ ¹³ and $\text{C}_4\text{C}_1\text{im}^+$ ¹⁴ cations. With this parameter set, we developed MM energy minimization and normal-mode calculation. In Tables 1, 2, and 3, we compare the most important configurational properties from the MM

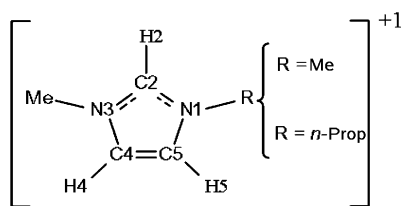


Figure 2. IUPAC nomenclature for the ring atoms of the imidazolium cations.

TABLE 1: Bond Lengths (in Å) from MM and QM Minimizations for the $\text{C}_1\text{C}_1\text{im}^+$ and $\text{C}_3\text{C}_1\text{im}^+$ Cations

bond	cation			
	$\text{C}_1\text{C}_1\text{im}^+$		$\text{C}_3\text{C}_1\text{im}^+$	
	QM	MM	QM	MM
C1'–N3	1.467	1.472	1.466	1.481
N1–C2	1.316	1.343	1.314	1.346
C2–N3	1.314	1.333	1.316	1.347
N3–C4	1.378	1.378	1.378	1.385
C4–C5	1.342	1.356	1.342	1.351
C5–N1	1.377	1.387	1.378	1.384
N1–C1'	1.469	1.471	1.477	1.483
N1–N3	2.151	2.185	2.153	2.209
C1'–C2'			1.527	1.534
C2'–C3'			1.529	1.531

TABLE 2: Bond Angles (in Degrees) from MM and QM Minimizations for the $\text{C}_1\text{C}_1\text{im}^+$ and $\text{C}_3\text{C}_1\text{im}^+$ Cations

angle	cation			
	$\text{C}_1\text{C}_1\text{im}^+$		$\text{C}_3\text{C}_1\text{im}^+$	
	QM	MM	QM	MM
C1'–N3–C2	125.7	127.4	126.4	129.8
C1'–N1–C2	126.4	127.6	126.2	129.9
C2'–C1'–N1			112.3	110.1
C3'–C2'–C1'			111.2	110.3
N1–C2–N3	109.8	109.4	109.9	110.2
C2–N3–C4	108.1	107.9	108.0	106.8
N3–C4–C5	107.0	107.9	107.0	108.1
C4–C5–N1	107.2	107.0	107.2	108.0
C5–N1–C2	108.0	107.7	107.9	106.9
total ring angle	540.1	539.9	540.0	540.0

TABLE 3: Main Dihedral Angles (in Degrees) from MM and QM Minimizations for the $\text{C}_3\text{C}_1\text{im}^+$ Cation

dihedral	QM	MM
C2'–C1'–N1–C2	98.95	95.22
C2'–C1'–N1–C5	79.08	82.63

TABLE 4: Dipole Moments μ (in D) from the RESP Model and QM Calculations for the Cations^a

	cation			
	$\text{C}_1\text{C}_1\text{im}^+$	$\text{C}_2\text{C}_1\text{im}^+$	$\text{C}_3\text{C}_1\text{im}^+$	$\text{C}_4\text{C}_1\text{im}^+$
μ_{QM}	1.08	1.76	3.49	5.57
μ_{RESP}	1.09	1.78	3.51	5.61
$\Delta\mu$	0.01	0.02	0.02	0.04

^a $\Delta\mu$ indicates the difference between the RESP dipole and the QM dipole.

calculations with the corresponding QM results for the new cations. This comparison demonstrates that the set of parameters employed in the MM calculations provides geometrical parameters for the cations that agree satisfactorily with the QM findings. The normal-mode analysis from the MM computations furnishes frequencies that coincide with the QM results within the limits observed for the $\text{C}_2\text{C}_1\text{im}^+$ and $\text{C}_4\text{C}_1\text{im}^+$ cations.¹⁴ From these comparisons between MM and QM data, we conclude that the transfer of the potential parameters presented in refs 13 and 14 permits an adequate description for the two new cations.

From the optimized MM geometries and RESP point charges, we computed the gas phase dipole moments μ of the cations. In Table 4, we compare these dipoles with the QM results including also data for the $\text{C}_2\text{C}_1\text{im}^+$ and $\text{C}_4\text{C}_1\text{im}^+$ cations.¹⁴ The agreement between dipoles from the RESP charge model and the QM calculations is excellent (the RESP charge model predicts dipoles that are approximately 1% larger than the QM data) for the four cations. Thus, our point charge model based on the RESP procedures is very effective in reproducing the QM charge distribution for the imidazolium based cations. Moreover, the cation's dipole moment increases significantly with the cation's alkyl chain length. This behavior is expected due to the charge dispersion produced by the larger alkyl chains.

3.2. Densities and Internal Energies. The established force field for the cations has been employed in MD simulations of the corresponding ILs containing AlCl_4^- as the counterions. From these simulations, the effect of the alkyl chain length on the liquid state properties of the ILs is investigated. The density ρ of the ILs is probably the best known experimental property.

TABLE 5: Experimental (exp, from ref 41) and Computed (sim) Mass Densities ρ_m (in g/cm³) as Well as Computed Number Densities ρ_n (em mol/L³) for the ILs at Temperatures T (em K)^a

IL	T	ρ_m (exp)	ρ_m (sim)	ρ_n
C ₁ C ₁ imAlCl ₄	363	1.329	1.351(5)	4.957
C ₂ C ₁ imAlCl ₄	298	1.302	1.363(4)	4.423
C ₃ C ₁ imAlCl ₄	298	1.262	1.317(4)	4.276
C ₄ C ₁ imAlCl ₄	298	1.238	1.258(2)	4.020

^a Numbers in parentheses indicate the uncertainty in the last digit.**TABLE 6: Internal Energies U and Electrostatic U_{el} and van der Waals U_{vdw} Contributions from the MD Simulations in Units of kJ/mol^a**

IL	U_{el}	U_{vdw}	U
C ₁ C ₁ imAlCl ₄	-397.2 ± 9.9	-75.8 ± 0.6	-473.0 ± 10.0
C ₂ C ₁ imAlCl ₄	-399.0 ± 8.5	-86.7 ± 0.4	-485.7 ± 8.4
C ₃ C ₁ imAlCl ₄	-393.2 ± 7.3	-91.8 ± 0.4	-485.0 ± 7.4
C ₄ C ₁ imAlCl ₄	-375.4 ± 10.4	-92.0 ± 3.7	-467.4 ± 12.1

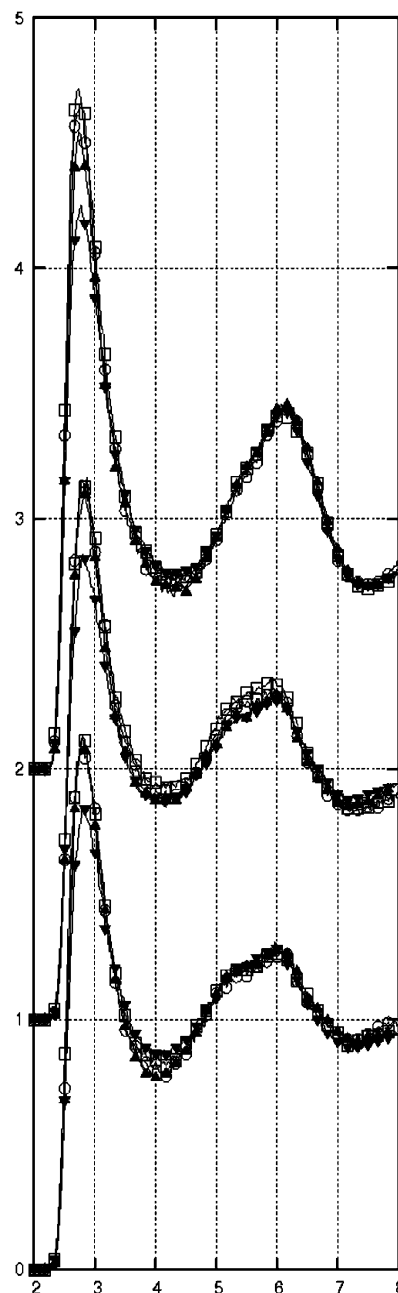
^a The simulation temperatures are 298 K with the exception of the IL C₁C₁imAlCl₄ (363 K).

In terms of MD simulations, ρ is acquired within the NpT ensemble.⁴⁰ Thus, the density is calculated generally in simulation studies focusing on the validation of new force field parameters. In the case of the C₂C₁imAlCl₄¹³ and C₄C₁imAlCl₄¹⁴ ILs, our group already confirmed that the force field approach presented above yields liquid state densities reproducing the experimental findings.

In Table 5, we summarized the mass ρ_m and number densities ρ_n of the four ILs obtained from NpT simulations at 1 atm and temperatures where experimental densities are available.⁴¹ Comparing with the experimental mass densities, we find an excellent agreement for all of the studied ILs with deviations below the acceptable limit of 5%. Although the IL C₁C₁imAlCl₄ was simulated at a higher temperature, the effect of the alkyl chain length becomes evident from the data in Table 5. Increasing the alkyl group from methyl ($n = 1$) to butyl ($n = 4$), a gradual decrease in ρ_m and ρ_n is observed. Thus, larger alkyl chains reduce the density of the IL which may be interpreted as a steric effect on the liquid state's ion configurations. This tendency has also been observed in simulation studies on ILs containing the Cl[−] and BF₄[−] anions.²³

Another important property of the ILs is represented by the internal energy U . The computed internal energies as well as its contributions originated at electrostatic U_{el} and van der Waals U_{vdw} interactions are presented in Table 6 for the four ILs. Comparing these data for the four ILs, we observe less negative internal energies in ILs with larger alkyl groups. Note that the IL C₁C₁imAlCl₄ has been simulated at a significantly higher temperature than the other ILs. As expected, by adding additional van der Waals centers to the cations, the van der Waals portion U_{vdw} increases (becomes more negative) when the side chain is increased. However, the opposite tendency is observed in the dominant electrostatic contribution U_{el} . On the other hand, in simulation studies on Cl[−] and BF₄[−] containing ILs from a united atom force field, the van der Waals term has been characterized to determine the chain length dependence of U .²³

3.3. Hydrogen Bonding. The liquid structure represents an important subject in most of the published simulation studies on ILs. With respect to details on structural organization in the AlCl₄[−] containing ILs, we refer the interested to ref 17. Microscopic structural details in other ILs have been published

**Figure 3.** RDFs for distances between the imidazolium ring hydrogens and the chlorine atoms. Illustrated are the RDFs for the H5 atom (not shifted, bottom curves), the H4 atom (shifted by 1), and the H2 atom (shifted by 2, top curves) in the ILs C₁C₁imAlCl₄ (down triangles), C₂C₁imAlCl₄ (up triangles), C₃C₁imAlCl₄ (open circles), and C₄C₁imAlCl₄ (open squares).

in ref 42. In the present manuscript, we investigate in detail the alkyl chain length effect on the trend of forming hydrogen bonds in this class of ILs. The charge distribution for the cations (see Figure 1) reveals positively charged imidazolium ring hydrogens that might coordinate strongly to negatively charged atoms of the anions (here, the chlorine atoms of the AlCl₄[−] anions).¹⁷

In our ILs, we distinguish the three ring hydrogens by the commonly adopted annotation H2, H4, and H5 (see Figure 2). The H2 hydrogen represents the substituent at the carbon between the two nitrogens. The H4 hydrogen is the substituent at the ring carbon close to the methyl group, whereas H5 denotes the hydrogen substituent at the ring carbon in the vicinity of the alkyl group. In Figure 3, we depicted the RDFs for distances

TABLE 7: Peak Positions r (in Å) and Integrals I for the First Peaks in the RDFs from Figure 2^a

IL	H2-Cl		H4-Cl		H5-Cl	
	r	I	r	I	r	I
C ₁ C ₁ imAlCl ₄	2.78	4.16	2.83	3.05	2.83	3.11
C ₂ C ₁ imAlCl ₄	2.78	3.81	2.83	3.33	2.78	3.11
C ₃ C ₁ imAlCl ₄	2.78	3.75	2.83	3.11	2.78	2.79
C ₄ C ₁ imAlCl ₄	2.73	3.41	2.83	3.05	2.83	2.84

^a Note that the simulation temperatures are 298 K with the exception of the IL C₁C₁imAlCl₄ (363 K).

between the ring hydrogens H2, H4, and H5 and the chlorine atoms of the anions.

At a glance, all of the functions from Figure 3 exhibit similar shapes, forming a first peak with maxima around 2.80 Å and a second peak around 6 Å. Apparently, the functions describing the H2-Cl distances possess larger first peak amplitudes than the RDFs for the H4-Cl and H5-Cl distances. To analyze the differences between the RDFs, we present the positions and integrals corresponding to coordination numbers for the first peak in Table 7.

The first peak in the RDF for H2-Cl distances is slightly shifted toward smaller distances than for the H4-Cl and H5-Cl distances. Also, the H2-Cl coordination is stronger than the H4-Cl and H5-Cl coordinations, as indicated by the significant larger integrals. This is in agreement with other simulation studies on imidazolium based ionic liquids.^{23,43} Differences between the RDFs for H4-Cl and H5-Cl are smaller when compared to the H2-Cl RDFs.

The first maxima in the H2-Cl RDFs from Figure 3 increase in amplitude with increasing alkyl chain length accompanied by a small reduction in the peak broadening, as indicated by the gradually decreasing coordination numbers (4.16 for C₁C₁imAlCl₄, 3.41 for C₄C₁imAlCl₄). Because the average coordination to more than three chlorine atoms of the same AlCl₄⁻ anion is impossible, these rather large integrals indicate the coordination of more than a single AlCl₄⁻ anion at each H2 site. The peak sharpening and increase in amplitude point to more localized and less mobile anions in ILs with larger alkyl chains at the H2 hydrogen.

The vicinity of the H4 and H5 hydrogens permits anion sharing. The obtained coordination numbers are slightly larger for the H4 site, indicating that the alkyl group represents somehow a steric hindrance for anion coordination at H5. Although weaker, the decrease in the coordination numbers with increasing alkyl chain follows the tendency described above for H2.

We have performed additional ab initio QM calculations at different levels of theory on ion pairs composed by the C_{*n*}C₁im⁺ cations ($n = 1, 2, 3, 4$) and the AlCl₄⁻ anion placed close to the preferential H2 hydrogen of the cations. In Table 8, we present the obtained H2-Cl distances from the optimized ion pair geometries. All of the QM distances compare fairly well among each other and with the H2-Cl distance of 2.67 Å computed for the C₂C₁imAlCl₄ ion pair at the RHF//6-311G(d) level of theory.⁴⁴ From the distances in Table 8, it becomes evident that the length of the alkyl group does not affect this structural parameter in the ILs.

All of the ab initio calculations exhibit ion pair geometries with three chlorine atoms coordinating to the H2 hydrogen and C2-H2-Cl angles close to 150°. In addition, in the ion pairs, the Al atom is slightly shifted out of the ring plane. In the MD simulations, the coordinating AlCl₄⁻ anions at the H2 hydrogen

TABLE 8: H2-Cl Distances (in Å) for the C_{*n*}C₁imAlCl₄ Ion Pairs Obtained from RHF ab initio Calculations at Several Levels of Theory^a

IL	RDF	6-31G(d)	6-31G(d,p)	6-311G(d,p)
C ₁ C ₁ imAlCl ₄	2.78	2.692	2.680	2.767
C ₂ C ₁ imAlCl ₄	2.78	2.685	2.674	2.724
C ₃ C ₁ imAlCl ₄	2.78	2.691	2.679	2.722
C ₄ C ₁ imAlCl ₄	2.74	2.692	2.680	2.723

^a The first column (RDF) indicates the peak position of the first maximum in the corresponding RDF for distances between the H2 and chlorines from Table 7.

TABLE 9: RHF//6-31G(d) Energies for the Cations E_{cat} and Interaction Energies for the Ion Pairs E_{int} ^a

IL	E_{cat}	E_{int}	Δq_{RESP}	Δq_{ChelpG}
C ₁ C ₁ imAlCl ₄	-303.27379	-0.10969	-0.1403	-0.0841
C ₂ C ₁ imAlCl ₄	-342.31342	-0.10827	-0.1398	-0.0869
C ₃ C ₁ imAlCl ₄	-381.34946	-0.10767	-0.1413	-0.0913
C ₄ C ₁ imAlCl ₄	-420.38474	-0.10727	-0.1397	-0.0893

^a Also included are the net charge transfers Δq from the anions to the cations obtained from RESP and ChelpG methodologies. Energies are given in hartrees and charges in units of e . The energy of the AlCl₄⁻ anion at this level of theory is -2080.23047 hartree.

have been detected to sit slightly above and below the imidazolium ring¹⁷ in agreement with the ab initio results. Quite general, ab initio pair geometries are expected to differ from the nearest neighbor liquid state configuration obtained from MD simulations as a consequence of density effects, particularities in the many-body neighborhood of the liquid state, or nonadequate hydrogen bonding description by the employed force field. Thus, the observed coincidence in ab initio and liquid state ion pair structures is surprising, even if one considers that discrepancies have been observed in MD results for other ILs. We mention the case of C₁C₁imCl, where probability densities for finding the Cl⁻ anion around the C₁C₁im⁺ cations differ when results from classical simulation techniques^{43,45,46} are compared with data from ab initio MD methodologies,⁴⁷⁻⁴⁹ QM ion pair calculations,⁵⁰ and experimental neutron diffractions studies.⁵¹

To further investigate the interaction of cations and anions in the four ILs, we compare the ion pair interaction energies between cations and the AlCl₄⁻ anion as well as the degree of charge transfer from the anions to the cations at the QM level in Table 9. Note that the data from this table have been computed from optimized geometries at the RHF//6-31G(d) level for the ion pairs described above. The interaction energies are not corrected for basis size superposition effects and zero point energies. The optimized geometries present the distances H2-Cl from Table 8 with almost 150° angles for the C2-H2-Cl configurations. Thus, the computed interaction energies from Table 9 clearly evidence the presence of hydrogen bonds in the ion pairs. The charge transfer from the anion to the cation was calculated by the molecular electrostatic potential methodologies RESP³⁴ and ChelpG⁵² (with the Gaussian 98 program).⁵³ Both methods indicate a charge transfer from the anion to the cation producing the net cation charge 0.91-0.95 e with the ChelpG and 0.85 e with the RESP methodology in the examined ILs. We are not able to correlate the degree of charge transfer with the length of the alkyl chain but observed slightly weakened interactions between cations and anions with growing alkyl groups.

3.4. Kitaura-Morokuma Partition. In Table 10, we resume our results for the Kitaura-Morokuma energy partition outlined

TABLE 10: Kitaura–Morokuma Energy Partition from eq 1 for the Interaction of the Cations and the AlCl_4^- Anions in the ILs at Various Levels of *ab initio* RHF Calculations^a

energy term	basis	$\text{C}_1\text{C}_1\text{im}^+$	$\text{C}_2\text{C}_1\text{im}^+$	$\text{C}_3\text{C}_1\text{im}^+$	$\text{C}_4\text{C}_1\text{im}^+$
$E_{\text{A-B}}$	6-31G(d)	−293.7	−290.0	−288.6	−287.5
	6-31G(d,p)	−294.1	−290.4	−288.9	−287.9
	6-311G(d,p)	−293.3	−289.3	−288.0	−286.9
E_{ES}	6-31G(d)	−301.7	−296.5	−294.2	−292.8
	6-31G(d,p)	−302.1	−297.1	−294.9	−293.4
	6-311G(d,p)	−300.3	−294.9	−292.6	−291.1
E_{EX}	6-31G(d)	32.1	32.4	32.1	32.0
	6-31G(d,p)	32.8	33.2	32.9	32.8
	6-311G(d,p)	30.5	30.8	30.9	30.8
$E_{\text{PL,cation}}$	6-31G(d)	−6.7	−7.7	−8.2	−8.5
	6-31G(d,p)	−6.9	−7.8	−8.3	−8.6
	6-311G(d,p)	−6.8	−7.7	−8.2	−8.5
$E_{\text{PL,anion}}$	6-31G(d)	−11.0	−10.8	−10.7	−10.6
	6-31G(d,p)	−11.1	−10.8	−10.7	−10.6
	6-311G(d,p)	−10.9	−10.5	−10.5	−10.4
$E_{\text{PL,Mix}}$	6-31G(d,p)	−2.3	−2.6	−2.6	−2.7
	6-31G(d)	−2.4	−2.6	−2.6	−2.7
	6-311G(d,p)	−2.3	−2.4	−2.6	−2.6
$E_{\text{PL,total}}$	6-31G(d)	−20.1	−21.0	−21.5	−21.7
	6-31G(d,p)	−20.4	−21.2	−21.6	−21.9
	6-311G(d,p)	−20.0	−20.7	−21.3	−21.5
$E_{\text{CT,cation}}$	6-31G(d)	−1.5	−1.4	−1.4	−1.4
	6-31G(d,p)	−1.6	−1.6	−1.5	−1.5
	6-311G(d,p)	−1.8	−1.8	−1.8	−1.8
$E_{\text{CT,anion}}$	6-31G(d)	−7.7	−8.4	−8.5	−8.4
	6-31G(d,p)	−8.1	−8.7	−8.7	−8.7
	6-311G(d,p)	−6.9	−7.4	−7.8	−7.7
$E_{\text{CT,total}}$	6-31G(d)	−9.3	−9.8	−9.8	−9.8
	6-31G(d,p)	−9.7	−10.3	−10.3	−10.2
	6-311G(d,p)	−8.7	−9.2	−9.5	−9.5
E_{Mix}	6-31G(d)	5.2	4.9	4.8	4.8
	6-31G(d,p)	5.3	5.1	5.0	4.9
	6-311G(d,p)	5.1	4.7	4.5	4.4

^a The energies are given in kJ/mol.

by eq 1 for the interactions of the $\text{C}_n\text{C}_1\text{im}^+$ cations ($n = 1, 2, 3, 4$) with the AlCl_4^- anion for the ion pairs described above. The computed energy contributions demonstrate that the most important term is the electrostatic interaction of the charge distributions E_{ES} , as expected for the interaction of two ions with opposite net charges. This interaction is more attractive than the overall interaction energy $E_{\text{A-B}}$. The exchange-repulsion term E_{EX} is approximately 11% of the total interaction energy. Table 10 also shows that polarization $E_{\text{PL,total}}$ is more important than charge transfer $E_{\text{CT,total}}$. The higher order coupling term E_{Mix} represents a small repulsive interaction in any case. These general considerations are not affected by the basis sets employed in the RHF calculations.

Increasing the alkyl group weakens the total interaction energy by 3.7–4.0 kJ/mol going from methyl to ethyl and by 1.0–1.5 kJ/mol for adding additional CH_2 groups. The tendency of weakening the interaction between cation and anion is very similar in the leading electrostatic portion E_{ES} . On the other hand, the exchange-repulsion term E_{EX} is not influenced by the length of the alkyl chain.

The polarization energy $E_{\text{PL,total}}$ contributes approximately 7% to the total interaction energy. In contrast to the energy portions discussed before, this term becomes more attractive by approximately 0.4 kJ/mol if one adds a CH_2 group to the alkyl chain. Roughly half of the polarization energy is due to polarization in the anion $E_{\text{PL,anion}}$ independent of the alkyl group in the polarizing cation. Simultaneous polarization $E_{\text{PL,Mix}}$ is small. For the polarization effects in the cation $E_{\text{PL,cation}}$ due to

electric fields created by the AlCl_4^- anions, we observe the increased interaction in ion pairs with cations that contain larger alkyl groups.

The charge transfer term $E_{\text{CT,total}}$ produces approximately 3% of the total interaction energy. As expected, this term is dominated by the contribution $E_{\text{CT,anion}}$ describing the transfer of electron density from the anion to the cation. Our calculations do not exhibit a distinct tendency for the charge transfer interaction energy when the length of the alkyl group is varied.

4. Conclusions

In the present manuscript, we extended our force field for liquid state simulation in dialkylimidazolium based ILs^{13,14} by including the cations 1,3-dimethyl- and 1-propyl-3-methylimidazolium. The obtained force field parameters for these two cations fit perfectly into the previously published parametrization of other 1-alkyl-3-methylimidazolium cations using the AMBER prescription corroborating the transferability of our force field within this class of ILs.

Performing MD simulations, the ILs $\text{C}_n\text{C}_1\text{imAlCl}_4$ with $n = 1, 2, 3, 4$ were studied with the objective to extract the effect of the n -alkyl group length on the liquid's density, internal energies, and hydrogen bonding behavior. We found that both the mass density and the number density in these ILs decrease when the alkyl chain is increased. The same tendency has been observed in the internal energies of the ILs and its electrostatic contribution. However, van der Waals interactions become more attractive when the alkyl group is increased.

Hydrogen bonding of the chlorine atoms to the hydrogens connected with the imidazolium ring has been revealed by RDFs in the liquid state. As in other ILs, the hydrogen bonding is more pronounced at the H2 hydrogens than at the H4 and H5 hydrogens.

We utilized *ab initio* calculations at the RHF level on the ion pairs composed by the $\text{C}_n\text{C}_1\text{im}^+$ cations and AlCl_4^- anions placed close to the H2 hydrogen of the cations. These calculations revealed that the H2–Cl distance detected in the liquid state can be interpreted as hydrogen bonding. Both the liquid state simulations and the QM calculations present weaker hydrogen bonding in ILs composed by cations with longer n -alkyl groups.

If we consider the energy partition within the Kitaura–Morokuma scheme in attempts to improve classical force fields, it appears to be more appropriate to include polarization interactions than charge transfer effects, at least for ILs containing the AlCl_4^- anion.

Acknowledgment. We wish to thank the Brazilian agency CNPq for financial support (476661/2006-4 and 301837/2006-6) and a scholarship for E.S.B.

References and Notes

- (1) Horvath, I. T.; Anastas, P. T. *Chem. Rev.* **2007**, *107*, 2169.
- (2) Jessop, P.; Leitner, W. *Chemical Synthesis Using Supercritical Fluids*; Wiley-VCH: Weinheim, Germany, 2007.
- (3) Horvath, I. T. *Acc. Chem. Res.* **1998**, *31*, 641.
- (4) *Ionic Liquids IIIA/B: Fundamentals, Progress, Challenges, and Opportunities*; Rogers, R. D., Seddon, K. R., Eds.; ACS Symp. Ser. 901/902; American Chemical Society: Washington, DC, 2005.
- (5) *Ionic Liquids in Synthesis*; Wasserscheid, P., Welton, T., Eds.; Wiley-VCH: Weinheim, Germany, 2003.
- (6) Zaitsau, D. H.; Kabo, G. J.; Strechan, A. A.; Paulechka, Y. U.; Tschersich, A.; Verevkin, S. P.; Heintz, A. *J. Phys. Chem. A* **2006**, *110*, 7303.
- (7) Earle, M. J.; Esperança, J. M. S. S.; Gilea, M. A.; Canongia Lopes, J. N.; Rebelo, L. P. N.; Magee, J. W.; Seddon, K. R.; Widegren, J. A. *Nature* **2006**, *439*, 831.

- (8) Emel'yanenko, V. N.; Verevkin, S. P.; Heintz, A. *J. Am. Chem. Soc.* **2007**, *129*, 3930.
- (9) Wishart, J. F.; Castner, E. W., Jr. Recent advances on experimental techniques applied to ILs are summarized in: *J. Phys. Chem. B* **2007**, *111*, 4639. And other articles from the special edition on The Physical Chemistry of Ionic Liquids: *J. Phys. Chem. B* **2007**, *111* (18).
- (10) For a summary of the classical simulation methodologies applied to imidazolium based ILs, see: Hunt, P. A. *Mol. Simul.* **2006**, *32*, 1.
- (11) Hunt, P. A.; Gould, I. R.; Kirchner, B. Correlations of physical-chemical properties with QM results. *Aust. J. Chem.* **2007**, *60*, 9.
- (12) Ludwig, R. *Phys. Chem. Chem. Phys.* **2008**, *10*, 4333.
- (13) de Andrade, J.; Böes, E. S.; Stassen, H. *J. Phys. Chem. B* **2002**, *106*, 3546.
- (14) de Andrade, J.; Böes, E. S.; Stassen, H. *J. Phys. Chem. B* **2002**, *106*, 13344.
- (15) de Andrade, J.; Böes, E. S.; Stassen, H. In *Ionic Liquids IIIA/B: Fundamentals, Progress, Challenges, and Opportunities*; Rogers, R. D., Seddon K. R., Eds.; ACS Symp. Ser. 901/902; American Chemical Society: Washington, DC, 2005; p 118.
- (16) Cornell, W. D.; Cieplak, P.; Bayly, C. I.; Gould, I. R.; Merz, K. M.; Ferguson, D. M.; Spellmeyer, D. C.; Fox, T.; Caldwell, J. W.; Kollman, P. A. *J. Am. Chem. Soc.* **1995**, *117*, 5179.
- (17) de Andrade, J.; Böes, E. S.; Stassen, H. *J. Phys. Chem. B* **2008**, *112*, 8966.
- (18) Dupont, J. *J. Braz. Chem. Soc.* **2004**, *15*, 341.
- (19) Triolo, A.; Russina, O.; Bleif, H. J.; Di Cola, E. *J. Phys. Chem. B* **2007**, *111*, 4641.
- (20) Wang, Y.; Voth, G. A. *J. Am. Chem. Soc.* **2005**, *127*, 12192.
- (21) Wang, Y.; Voth, G. A. *J. Phys. Chem. B* **2006**, *110*, 18601.
- (22) Canongia Lopes, J. N. A.; Pádua, A. A. H. *J. Phys. Chem. B* **2006**, *110*, 3330.
- (23) Raabe, G.; Köhler, J. *J. Chem. Phys.* **2008**, *128*, 154509.
- (24) Hardacre, C.; Holbrey, J. D.; McCormac, P. B.; McMath, S. E. J.; Nieuwenhuyzen, M.; Seddon, K. R. *J. Mater. Chem.* **2001**, *11*, 346.
- (25) Downard, A.; Earle, M. J.; Hardacre, C.; McMath, S. E. J.; Nieuwenhuyzen, M.; Teat, S. J. *Chem. Mater.* **2004**, *16*, 43.
- (26) Binnemans, K. *Chem. Rev.* **2005**, *105*, 4148.
- (27) Dobbs, W.; Douce, L.; Allouche, L.; Louati, A.; Malbosc, F.; Welter, R. *New J. Chem.* **2006**, *30*, 528.
- (28) Yan, T.; Burnham, C. J.; Del Pópolo, M. G.; Voth, G. A. *J. Phys. Chem. B* **2004**, *108*, 11877.
- (29) Zhao, W.; Eslami, H.; Cavalcanti, W. L.; Müller-Plathe, F. *Z. Phys. Chem.* **2007**, *221*, 1647.
- (30) Chaumont, A.; Schurhammer, R.; Wipff, G. *J. Phys. Chem. B* **2005**, *109*, 18964.
- (31) Bhargava, B. L.; Balasubramanian, S. *J. Chem. Phys.* **2007**, *127*, 114510.
- (32) Kitaura, K.; Morokuma, K. *Int. J. Quantum Chem.* **1976**, *10*, 325.
- (33) Schmidt, M. W.; Baldrige, K. K.; Boatz, J. A.; Elbert, S. T.; Gordon, M. S.; Jensen, J. H.; Koseki, S.; Matsunaga, N.; Nguyen, K. A.; Su, S. J.; Windus, T. L.; Dupuis, M.; Montgomery, J. A. *J. Comput. Chem.* **1993**, *14*, 1347.
- (34) Bayly, C. I.; Cieplak, P.; Cornell, W. D.; Kollman, P. A. *J. Phys. Chem.* **1993**, *97*, 10269.
- (35) Pappu, R. V.; Hart, R. K.; Ponder, J. W. *J. Phys. Chem. B* **1998**, *102*, 9725. Dudek, M. J.; Ramnarayan, K.; Ponder, J. W. *J. Comput. Chem.* **1998**, *19*, 548.
- (36) Lyubartsev, A. P.; Laaksonen, A. *Comput. Phys. Commun.* **2000**, *128*, 565.
- (37) Nosé, S. *Mol. Phys.* **1984**, *52*, 525.
- (38) Tuckerman, M.; Berne, B. J. *J. Chem. Phys.* **1992**, *97*, 1990.
- (39) Ewald, P. *Ann. Phys.* **1921**, *64*, 253.
- (40) Allen, M. P.; Tildesley, D. J. *Computer Simulation of Liquids*; Clarendon Press: Oxford, U.K., 1987.
- (41) Fannin, A. A., Jr.; Floreani, D. A.; King, L. A.; Landers, J. S.; Piersma, B. J.; Stech, D. J.; Vaughn, R. L.; Wilkes, J. S.; Williams, J. L. *J. Phys. Chem.* **1984**, *88*, 2614.
- (42) Qiao, B.; Krekeler, C.; Berger, R.; Delle Site, L.; Holm, C. *J. Phys. Chem. B* **2008**, *112*, 1743.
- (43) Urahata, S. M.; Ribeiro, M. C. C. *J. Chem. Phys.* **2004**, *120*, 1855.
- (44) Takahashi, S.; Suzuya, K.; Kohara, S.; Koura, N.; Curtiss, L. A.; Saboungi, M. L. *Z. Phys. Chem.* **1999**, *209*, 209.
- (45) Hanke, C. G.; Price, S. L.; Lynden-Bell, R. M. *Mol. Phys.* **2001**, *99*, 801.
- (46) Liu, Z.; Haung, S.; Wang, W. *J. Phys. Chem. B* **2004**, *108*, 12978.
- (47) Bühl, M.; Chaumont, A.; Schurhammer, R.; Wipff, G. *J. Phys. Chem. B* **2005**, *109*, 18591.
- (48) Del Pópolo, M. G.; Lynden-Bell, R. M.; Kohanoff, J. *J. Phys. Chem. B* **2005**, *109*, 5895.
- (49) Bhargava, B. L.; Balasubramanian, S. *Chem. Phys. Lett.* **2006**, *417*, 486.
- (50) Hunt, P. A.; Gould, I. R. *J. Phys. Chem. A* **2006**, *110*, 2269.
- (51) Hardacre, C.; Holbrey, J. D.; McMath, S. E.; Bowron, D. T.; Soper, A. K. *J. Chem. Phys.* **2003**, *118*, 273.
- (52) Breneman, C. M.; Wiberg, K. B. *J. Comput. Chem.* **1990**, *11*, 361.
- (53) Frisch, M. J.; Trucks, G. W.; Schlegel, H. B.; Scuseria, G. E.; Robb, M. A.; Cheeseman, J. R.; Zakrzewski, V. G.; Montgomery, J. A., Jr.; Stratmann, R. E.; Burant, J. C.; Dapprich, S.; Millam, J. M.; Daniels, A. D.; Kudin, K. N.; Strain, M. C.; Farkas, O.; Tomasi, J.; Barone, V.; Cossi, M.; Cammi, R.; Mennucci, B.; Pomelli, C.; Adamo, C.; Clifford, S.; Ochterski, J.; Petersson, G. A.; Ayala, P. Y.; Cui, Q.; Morokuma, K.; Malick, D. K.; Rabuck, A. D.; Raghavachari, K.; Foresman, J. B.; Cioslowski, J.; Ortiz, J. V.; Baboul, A. G.; Stefanov, B. B.; Liu, G.; Liashenko, A.; Piskorz, P.; Komaromi, I.; Gomperts, R.; Martin, R. L.; Fox, D. J.; Keith, T.; Al-Laham, M. A.; Peng, C. Y.; Nanayakkara, A.; Challacombe, M.; Gill, P. M. W.; Johnson, B.; Chen, W.; Wong, M. W.; Andres, J. L.; Gonzalez, C.; Head-Gordon, M.; Replogle, E. S.; Pople, J. A. *Gaussian 98*; Gaussian, Inc.: Pittsburgh, PA, 1998.